Available online at www.sciencedirect.com
ScienceDirect
Metabolism Clinical and Experimental 59 (2010) 1691 – 1700
Metabolism
Clinical and Experimental
www.metabolismjournal.com

Complementation of the metabolic defect in CTP:phosphoethanolamine cytidylyltransferase (*Pcyt2*)–deficient primary hepatocytes

Morgan D. Fullerton, Marica Bakovic*

Department of Human Health and Nutritional Sciences, University of Guelph, Guelph, Ontario, N1G 2W1, Canada N1G 2W1

Received 1 January 2010; accepted 30 March 2010

Abstract

The CTP:phosphoethanolamine cytidylyltransferase gene (*Pcyt2*) regulates the synthesis of CDP-ethanolamine, which is combined with diacylglycerol (DAG) to form the membrane phospholipid phosphatidylethanolamine (PE) via the de novo Kennedy pathway. [^{14}C] Ethanolamine and [^{3}H]glycerol radiolabeling experiments established that PE synthesis and turnover are reduced in primary hepatocytes isolated from *Pcyt2*-deficient (*Pcyt2*$^{+/-}$) mice relative to littermate controls. [^{3}H]Glycerol radiolabeling revealed an increased formation of both DAG and triglyceride (TAG) and only increased turnover of DAG, consistent with elevated TAG accumulation. [^{3}H]Acetate radiolabeling showed that de novo fatty acid (FA) synthesis also increased in *Pcyt2*-deficient hepatocytes. Overexpression of a Myc/His-tagged *Pcyt2* complementary DNA into deficient hepatocytes increased Pcyt2 protein expression; normalized PE synthesis and turnover; and reduced FA, DAG, and TAG synthesis. Although increased *Pcyt2-myc/His* complementary DNA expression normalized lipid homeostasis, a Pcyt2 mutant with 60% catalytic activity (H244Y) was unable to normalize any of the parameters investigated. Only when PE synthesis was fully reestablished did the lipogenic gene expression and the formation of FA, DAG, and TAG revert to the levels of wild-type hepatocytes. These data unambiguously establish that the TAG accumulation present in *Pcyt2*-deficient hepatocytes is a direct consequence of *Pcyt2* gene deficiency and reduced functioning of the de novo Kennedy pathway.

1. Introduction

Phosphatidylethanolamine (PE) is the primary phospholipid on the inner leaflet of cellular membranes and has been shown to regulate various cellular processes including cytokinesis, coagulation, autophagy, and cell signaling [1]. There are 2 main synthetic pathways for the production of PE. Decarboxylation of phosphatidylserine mostly contributes to mitochondrial PE [2] and has been shown to become dominant in the absence of ethanolamine in vitro [3]. Phosphatidylethanolamine is predominantly synthesized de novo by the CDP-ethanolamine or PE-Kennedy pathway [4], where ethanolamine is first taken into the cells and phosphorylated by ethanolamine kinase. CTP:phosphoethanolamine cytidylyltransferase (*Pcyt2*, gene; Pcyt2, protein) then catalyzes the formation of CDP-ethanolamine through the addition of CTP to phosphoethanolamine; and finally, 1,2-diacylglycerol ethanolaminephosphotransferase adds CDP-ethanolamine to diacylglycerol (DAG) at the endoplasmic reticulum to form PE phospholipid.

The Pcyt2 protein was first purified in the 1970s from rat liver [5]; but work on subcellular localization and kinetic properties was performed in more recent years [6-9], showing that it is approximately 50 kd and a cytosolic protein that exists as a dimer [8,9]. In 1996, the yeast *Pcyt2* gene was first identified [10]; and the human complementary DNA (cDNA) was isolated by genetic complementation of a conditional ethanolamine auxotroph [11]. Rat [12] and mouse [13] *Pcyt2* genes were subsequently cloned. The cloning of yeast and human cDNA indicated that the encoded protein is a member of the cytidylyltransferase superfamily, having the characteristic CTP binding motif HXGH [11]. There also exists a single signature peptide motif typical of the cytidylyltransferase family, RTXGVSTT, which has been proposed to interact with the CTP site [14]. Pcyt2 is a unique cytidylyltransferase with 2

* Corresponding author. Animal Science and Nutrition Building, University of Guelph, Guelph, Ontario, Canada N1G 2W1. Tel.: +1 519 824 4120x53764; fax: +1 519 763 5902.
E-mail address: mbakovic@uoguelph.ca (M. Bakovic).

0026-0495/$ – see front matter © 2010 Elsevier Inc. All rights reserved.
doi:10.1016/j.metabol.2010.03.022

HXGH motifs defining 2 cytidylyltransferase domains, suggesting that this gene has likely emerged from a unique internal duplication event [11,14].

The mouse gene and cDNA were characterized by our laboratory [13], showing that the *Pcyt2* gene can be alternatively spliced. The full-length transcript (*Pcyt2α*) experiences a splicing event that is evolutionary conserved and results in the loss of exon 7. The spliced exon corresponds to an 18–amino acid peptide (^{180}PPHPTPAGDTLSSEVSSQ^{197}) that links the homologous N and C terminal domains; therefore, the shorter variant (*Pcyt2β*) lacks the so-called internal linker peptide. When cloned and expressed in mammalian cells, both *Pcyt2α* and *Pcyt2β* produce active enzymes; however, the K_m for phosphoethanolamine is 2-fold higher in the longer α splice variant compared with the shorter β form [15]. The *Pcyt2* gene is universally expressed, yet the *Pcyt2* promoter function and transcription could be down-regulated in cancer cells [16,17] and up-regulated in differentiating muscle cells [18].

Under normal conditions, the formation of CDP-ethanolamine by Pcyt2 is the rate-limiting step in the pathway [19]; but as could be expected, if either ethanolamine [20] or DAG [21] becomes less available, these substrates would also limit PE formation. Ethanolamine is specifically used by the PE-Kennedy pathway, whereas DAG is used not only for the biosynthesis of membrane phospholipids (PE and phosphatidylcholine [PC]) but also for the energy storage in the form of triglycerides (TAG). Therefore, DAG could serve as a critical substrate for the balancing of membrane biogenesis and energy metabolism. Although the second role of DAG is well characterized, the actual relationships between membrane phospholipids and energy metabolism are generally poorly understood. Recently, we have developed a mouse model in which the *Pcyt2* gene has been partially disrupted [22,23]. Heterozygous (*Pcyt2*$^{+/-}$) animals display an array of abnormalities associated with human metabolic syndrome, including modified membrane composition, liver steatosis, hypertriglyceridemia, obesity, and insulin resistance. These abnormalities are exacerbated with age and therefore may not be directly related to the reduced PE synthesis via the de novo pathway [22]. Here we test if the reduced flux through the PE-Kennedy pathway is directly responsible for the observed metabolic phenotype at the stage of complete disease development. Reduced CDP-ethanolamine formation and consequently PE synthesis via the PE-Kennedy pathway generate an excess of DAG intermediate that has to be removed or stored in the form of TAG that would require both metabolic and genetic adaptations. We propose that, at least in *Pcyt2*-deficient liver cells, the restoration of the PE-Kennedy pathway by the overexpression of *Pcyt2* cDNA would simultaneously reduce DAG levels and consequently TAG formation, and reestablish lipogenic gene expression as a mechanism to alleviate the *Pcyt2*$^{+/-}$ liver steatosis (nonalcoholic fatty liver) phenotype.

2. Experimental procedures

2.1. Isolation of Pcyt2-deficient hepatocytes

Primary hepatocytes were isolated from 32- to 36-week-old *Pcyt2*$^{+/-}$ mice and wild-type (*Pcyt2*$^{+/+}$) littermate controls as previously described [22]. Briefly, livers were perfused with an EGTA buffer (140 mmol/L NaCl, 6.7 mmol/L KCl, 10 mmol/L HEPES, and 50 μmol/L EGTA, pH 7.4) solution and then with a solution (67 mmol/L NaCl, 6.7 mmol/L KCl, 5 mmol/L $CaCl_2{\cdot}2H_2O$, and 100 mmol/L HEPES, pH 7.6) containing 0.5% collagenase through the inferior vena cava after the superior vena cava was clamped and the portal vein was cut. Hepatocyte viability was assessed using trypan blue exclusion, and cell number was counted using a hemocytometer (viability was always greater than 90%). Hepatocytes were plated on 6-well plates (1×10^5 cells per 60-mm dish) and allowed to attach for 2 to 4 hours, and then media (Williams medium E) and floating cells were removed and replaced with a complete media (Williams medium E with 10% fetal bovine serum and 1% antibiotic-antimyotic solution [Invitrogen, Burlington, Ontario, Canada]).

2.2. Cloning of the wild-type Pcyt2α and H244Y mutant

The cloning of fully functional wild-type *Pcyt2α*-myc/His cDNA was previously described [15]. Briefly, the coding regions of the mouse *Pcyt2* cDNA were polymerase chain reaction (PCR) amplified using primers that introduced *Eco*RV and *Xho*I restriction sites to the 5′ and 3′ end, respectively. The translation termination codons were deleted. The coding sequence was then amplified and subcloned into the pGEM-T Easy vector (Promega, Madison, WI), removed by restriction digestion with *Eco*RV and *Xho*I, and subcloned into the pcDNA4/myc-His vector. Cloning of the H244Y mutant was as follows: A mutation in the second putative active site conferring a Tyr at position 244 in place of a His (**H244Y**IGH) was introduced into the mouse *Pcyt2α*-myc/His cDNA. Overlapping PCR was used to alter the His to Tyr (cac→tat). The first reaction used a forward primer also containing a 5′ *Eco*RV site (primer A: 5′-gatatcgccgccaggatttgcggg-3′) and a mutant reverse primer (primer B: 5′-ccacgtgcccga**tat**agaacaggt-caaagg-3′), which yielded a 752–base pair (bp) fragment containing the mutation (shown in bold). The second reaction used a forward primer complementary to mutant primer B (primer C) and a more downstream reverse primer containing an 3′ *Xho*I site (primer D: 5′-ctcgaggt-caatctcccctccagg-3′), which yielded a 498-bp fragment. The 752- and 498-bp amplified PCR products were then combined and used as a template for a third PCR reaction with the most external primers A and D to yield a single 1250-bp product corresponding to the full-length *Pcyt2α* cDNA. The amplified fragment was cloned into a PCR vector, pGEM-T Easy vector (Promega); isolated by digestion with *Eco*RV and *Xho*I; and then subcloned into

the pcDNA4/myc-His mammalian vector (Invitrogen) to yield the clone *Pcyt2*-H244Y-myc. Sequencing of *Pcyt2*-H244Y-myc ensured that the correct mutation was present and that no other errors were introduced by PCR.

2.3. Transfection of primary hepatocytes

Primary hepatocytes isolated from 32- to 36-week-old $Pcyt2^{+/-}$ mice and littermate controls were incubated overnight in complete medium at 37°C and transfected the following day. After 16 to 20 hours, overnight culture medium was replaced with a fresh medium containing 50 μmol/L ethanolamine. Hepatocytes were transfected using JetPEI transfection reagent (Polyplus transfection; New York, NY), where 6 μL of JetPEI in 100 μL of 100 mmol/L NaCl was combined with 3 μg of plasmid DNA (*Pcyt2*-myc/His or *Pcyt2*-H244Y-myc/His) in 100 μL of 100 mmol/L NaCl; and the mixture was then incubated at room temperature for 30 minutes. A transfection mixture volume of 200 μL was added directly into 2 mL of culture medium for each well. Cells were then incubated for 48 hours in a medium containing 50 μmol/L ethanolamine, at which point labeling experiments commenced. As per manufacturer's instructions, to ensure batch-to-batch reproducibility of the JetPEI transfections, 64 ng of pRL-CMV *Renilla* luciferase vector (Promega) was cotransfected with 3 μg of Pcyt2 plasmids or empty pcDNA4 vector. The Pcyt2 expression was then compared with luciferase activity (1247 ± 96 relative light units per milligram protein) to confirm no variations in transfections.

2.4. Metabolic radiolabeling of primary hepatocytes

Radiolabeling experiments were conducted by using 0.1 μCi per well of [^{14}C]ethanolamine (55 Ci/mmol) and 2.5 μCi per well of [^{3}H]glycerol (20 Ci/mmol). Transfected hepatocytes from $Pcyt2^{+/-}$ and $Pcyt2^{+/+}$ mice were pulsed from 1 to 4 hours with [^{14}C]ethanolamine or [^{3}H]glycerol to determine the synthetic rates of PE, DAG, and TAG. Additional 24-hour labeling was performed to assess their pool sizes as described previously [17]. To determine the rates of PE, DAG, and TAG degradation, the pulse-chase experiments were performed with [^{3}H]glycerol radiolabeling. The $Pcyt2^{+/-}$ and $Pcyt2^{+/+}$ hepatocytes were pulsed for 2 hours, after which the medium was removed and replaced with medium containing an excess of unlabeled substrate (250 μmol/L glycerol) and collected after 1-, 2-, and 4-h chase. Hepatocytes were washed twice with ice-cold phosphate-buffered saline (PBS) and collected in 300 μL of PBS, where 50 μL was used for measurements of protein concentration and luciferase luminescence.

Total lipids were extracted by the method of Bligh and Dyer [24]. For [^{14}C]ethanolamine experiments, the radioactivity of water-soluble intermediates of the PE-Kennedy pathway (ethanolamine, phosphoethanolamine, and CDP-ethanolamine) was determined from the aqueous phase and PE from the organic (chloroform) phase. Ethanolamine, phosphoethanolamine, and CDP-ethanolamine were separated by thin-layer chromatography in a solvent system of methanol/0.5% NaCl/ammonia (50:50:5, vol/vol/vol). The radiolabeled PE was separated from other lipids in a solvent system of chloroform/methanol/acetic acid/water (25:15:4:2, vol/vol/vol/vol), and all were analyzed by liquid scintillation counting. For [^{3}H]glycerol radiolabeling, lipids were separated in a solvent system of heptane/isopropyl ether/acetic acid (60:40:3, vol/vol/vol); and radioactivity in total phospholipids, DAG, and TAG was determined by liquid scintillation counting.

Transfected hepatocytes from $Pcyt2^{+/-}$ and $Pcyt2^{+/+}$ mice were also radiolabeled with [^{3}H]acetate (4 hours, 2.5 μCi per well; 20 Ci/mmol). The lipid (chloroform) phase was saponified with 200 μL of ethanolic 0.5 mol/L NaOH for 3 hours at 70°C, and 200 μL of water was added after cooling. The saponifiable fraction (phospholipids, DAG, and TAG) was extracted 3 times with 500 μL of petroleum ether, separated by thin-layer chromatography, and analyzed as described above. The nonsaponifiable fraction (mainly cholesterol) was acidified with 300 μL of 6 N HCl, extracted 3 times with 500 μL of petroleum ether, evaporated to dryness, and resuspended in a constant volume of chloroform (200 μL); and radioactivity was determined by liquid scintillation counting.

2.5. Expression in COS-7 cells

COS-7 cells grown on 6-well plates were transfected with 2.5 μg of plasmid DNA for *Pcyt2*-myc/His (wild-type), *Pcyt2*-H244Y-myc (mutant), and empty control vector pcDNA4/myc-His using 10 μL of Lipofectamine (Invitrogen). After 48 hours, the mock-transfected, wild-type, and mutant protein expressions were determined by Western blotting; and their functional contribution to the PE-Kennedy pathway was determined by [^{14}C]ethanolamine radiolabeling (0.2 μCi per well, 55 Ci/mmol, 2 hours in the presence of 50 μmol/L unlabeled ethanolamine). Radiolabeled cells were washed twice in ice-cold PBS and collected by trypsinization, and PE and its water-soluble intermediates from the PE-Kennedy pathway were determined by the same methodology described above for hepatocytes. The enzyme activity of the transfected cells was also determined in vitro by measuring the conversion of [^{14}C]phosphoethanolamine to [^{14}C]CDP-ethanolamine from whole cell homogenates of mock, wild-type, and H244Y mutant overexpressing cells as previously described [23,25].

2.6. Western blotting

Primary hepatocytes and COS-7 cells were collected into cold lysis buffer (10 mmol/L Tris-HCl [pH 7.4], 1 mmol/L EDTA, and 10 mmol/L NaF) containing protease (1/10) and phosphatase (1/100) inhibitor cocktails (Sigma Aldrich, Oakville, Ontario, Canada) and lysed further with 2 freeze-thaw cycles. Lysates were centrifuged at 13 000 rpm for 10 minutes at 4°C to remove cell debris, and supernatant was transferred to a new tube. Protein concentration was determined using the BCA method (Pierce, Rockford, IL).

The protein lysates (25 μg) were resolved on 10% sodium dodecyl sulfate polyacrylamide gel electrophoresis and semidry transferred to a polyvinylidene difluoride membrane. Proper protein transfer and equal loading were verified using Ponceau S staining, after which membranes were blocked with 5% milk in 20 mmol/L Tris-HCl (pH 7.5), 500 mmol/L NaCl, 0.05% Tween-20 (TBS-T) for 1 hour at room temperature followed by overnight incubation at 4°C with either anti-Pcyt2 antibody (1:2000 in 5% milk–TBS-T) or anti-Myc antibody (Invitrogen) (1:5000 in 5% milk–TBS-T). The generation and validation of the anti-Pcyt2 antibody have been previously described [23]. After 3 wash steps (5-10 minutes), membranes were incubated with a goat anti-rabbit or goat anti-mouse secondary antibody for anti-Pcyt2 and anti-Myc, respectively (1:20 000), for 1 hour at room temperature and then visualized with enhanced chemiluminescence.

2.7. Lipogenic gene analyses

Pcyt2 heterozygous hepatocytes were isolated and 48-hour transfected as described above. RNA was extracted using Trizol (Invitrogen, USA), as per the manufacturer's instructions. First-strand cDNA synthesis and semiquantitative PCR were conducted as previously described [23], where all PCR reactions were analyzed in the linear phase and using optimal cycle conditions. All genes are expressed relative to β-actin and normalized to nontransfected heterozygous controls (primers and cycle conditions available upon request).

2.8. Statistical analyses

This study involved comparisons between hepatocytes isolated from $Pcyt2^{+/+}$ and $Pcyt2^{+/-}$ mice. The 4 types of hepatocytes used were (1) untransfected $Pcyt2^{+/+}$, (2) untransfected $Pcyt2^{+/-}$, (3) $Pcyt2^{+/-}$ transfected with *Pcyt2*α-wild-type plasmid, and (4) $Pcyt2^{+/-}$ transfected with *Pcyt2*-H244Y mutant. All data are reported as mean ± SEM. The statistical differences were determined by analysis of variance followed by a Tukey post hoc test, at $P < .05$. Differences relative to $Pcyt2^{+/+}$ hepatocytes (group 1) are represented by [a], and differences relative to $Pcyt2^{+/-}$ hepatocytes (group 2) are represented by [b]. All pairwise comparisons were performed by Student *t* test when differences were considered significant at $P < .05$ or lower.

3. Results

3.1. Characterization of the wild-type Pcyt2 and H244Y mutant in COS-7 cells

We transiently transfected the wild-type and H244Y mutant *Pcyt2* cDNA into COS-7 cells to determine the individual plasmid expression and the effect of the active site mutation on enzyme function. The protein expression was monitored by detection of the Myc-epitope present in both plasmids 48 hours posttransfection. As shown in Fig. 1A, both Pcyt2 constructs were similarly expressed; and when

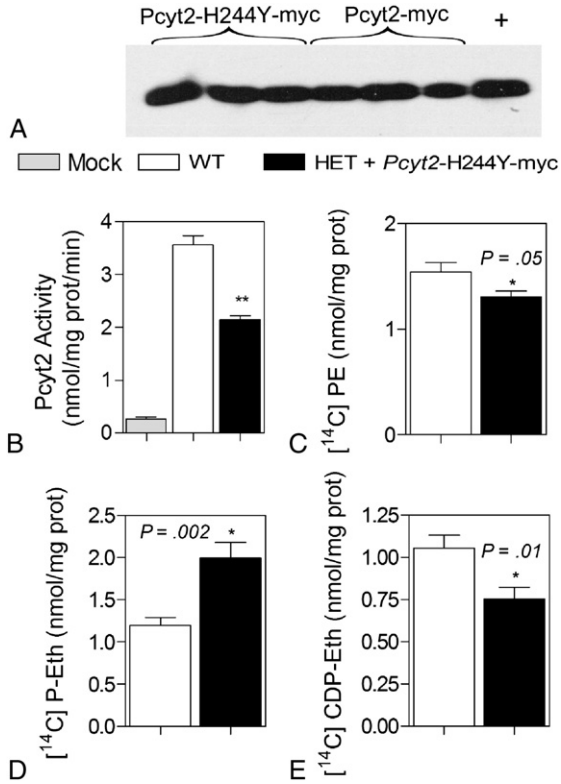

Fig. 1. Functional expression of the myc-tagged Pcyt2 and H244Y mutant. COS-7 cells were transfected for 48 hours with the wild-type *Pcyt2* (WT) or mutant (*Pcyt2 H244Y-myc*) and then radiolabeled with [^{14}C]ethanolamine for 2 hours. A, Anti-*myc* Western blots show a very similar level of expression of tagged proteins; (+) control is a pure *myc*-tagged Pcyt2 protein. B, Pcyt2 enzyme activity (in nanomoles per milligram protein per minute) was assessed in untransfected (mock) and transfected cells (WT-*Pcyt2-myc* and mutant-*Pcyt2 H244Y-myc*). Also shown are the amounts (in nanomoles per milligram protein) of the Kennedy pathway product [^{14}C] PE (C) and the pathway intermediates, [^{14}C]phosphoethanolamine (P-Eth) (D) and [^{14}C]CDP-ethanolamine (CDP-Eth) (E). All experiments were performed in triplicate (n = 3) and repeated at least 3 times. *P* values determined by Student *t* test, where ** represents $P < .01$.

enzyme activity was determined, the H244Y mutant had 40% lower activity than the wild-type *Pcyt2* (2.12 ± 0.02 vs 3.67 ± 0.16 nmol/[mg min]) (Fig. 1B). The expression was additionally tested in vivo by radiolabeling of the PE-Kennedy pathway with [^{14}C]ethanolamine. In agreement with the in vitro activity data, H244Y overexpressing cells had 15% reduced production of [^{14}C]PE (Fig. 1C), 40% increased radiolabeling of phosphoethanolamine (substrate) (Fig. 1D), and 25% decreased radiolabeling of CDP-ethanolamine (product) (Fig. 1E). These experiments demonstrated that both *Pcyt2* plasmids were functionally expressed and established that the H244Y mutant had reduced catalytic activity and function in the PE-Kennedy pathway. The significance of the second binding site in Pcyt2 was addressed by introducing a Tyr at amino acid position 244 in substitution of a His. Therefore, our results established the importance of the His within the second active site (HIGH) in the catalytic function of Pcyt2.

3.2. Functional analysis of the Pcyt2 wild-type and H244Y mutant in hepatocytes

Primary hepatocytes were isolated from 32- to 38-week-old heterozygous mice and control littermates. As in the COS-7 cells, hepatocytes were transiently transfected with *Pcyt2* plasmids and examined 48 hours later. Consistency in the expression of the wild-type and H244Y Pcyt2 constructs was ensured by monitoring the expressed proteins by immunoblotting using both Myc-tag (upper panel) and Pcyt2-specific (lower panel) antibodies (Fig. 2A). The endogenous level of Pcyt2 protein in untransfected

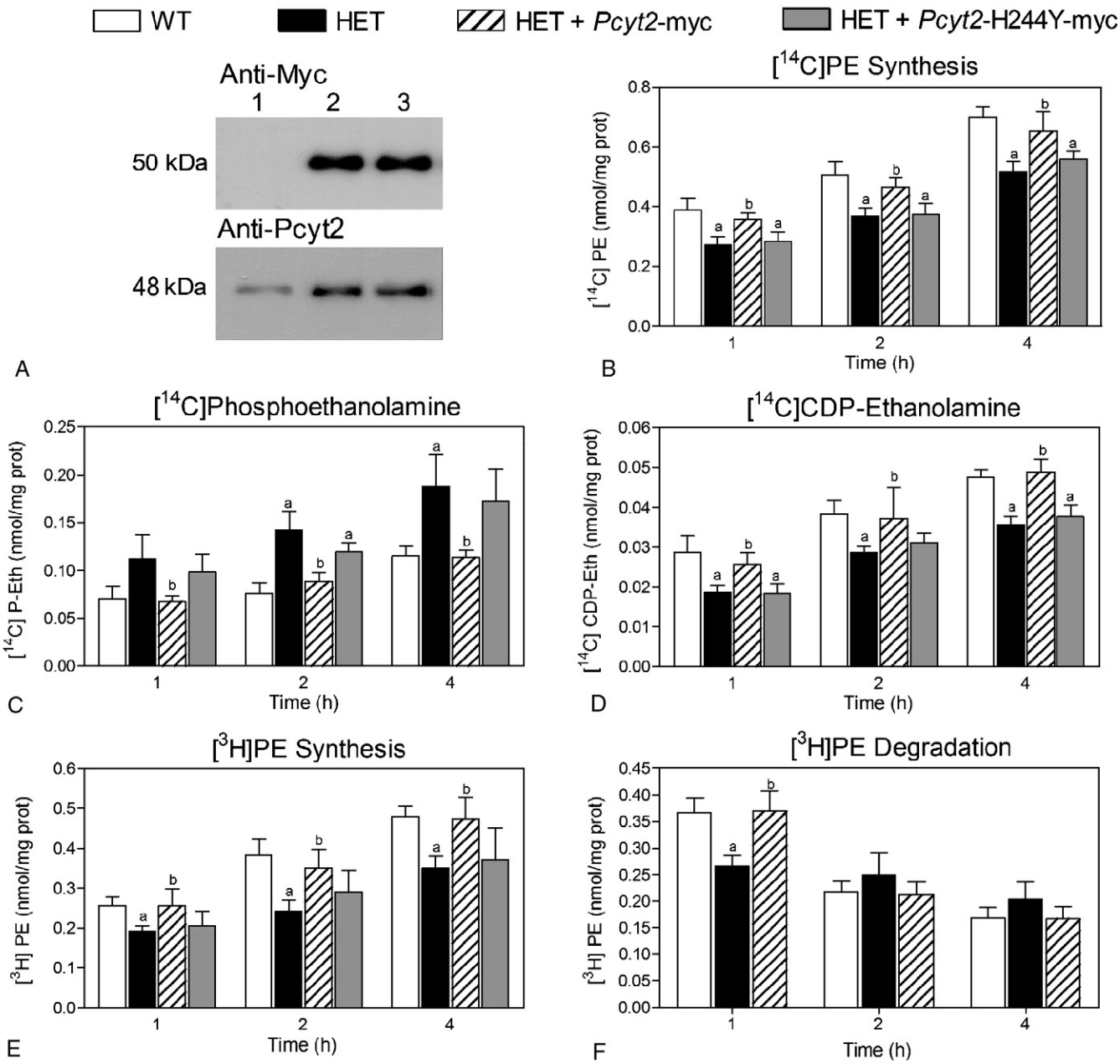

Fig. 2. Wild-type Pcyt2 but not H244Y mutant restores PE homeostasis. Control $Pcyt2^{+/+}$ (WT) and deficient $Pcyt2^{+/-}$ (HET) hepatocytes were transfected with either plasmid for 48 hours and then pulse labeled with [^{14}C]ethanolamine or [^{3}H]glycerol. A, Immunoblots demonstrating similar plasmid expression in deficient (HET) hepatocytes using anti-*myc* (above) and anti-Pcyt2 (below) antibodies (lane 1, nontransfected HET cells; lane 2, *Pcyt2*-H244Y-myc; lane 3, WT *Pcyt2*-myc transfected HET cells); the incorporation of [^{14}C]ethanolamine into PE (B), phosphoethanolamine (C), and CDP-ethanolamine (D) in transfected and untransfected HET and control WT hepatocytes. Hepatocytes were also pulse labeled with [^{3}H]glycerol to measure the incorporation of [^{3}H] into PE (synthesis) (E) or pulse-chased for PE degradation (F). Time points and types of transfection are indicated. All radiolabeling data are expressed as nanomoles per milligram protein. Hepatocytes from WT livers (n = 4) and HET livers (n = at least 4 transfected/4 nontransfected), where each time point was performed at least in triplicate. Significance was established at $P < .05$, where [a] represents a difference relative to WT and [b] represents a difference relative to HET cells as determined by ANOVA.

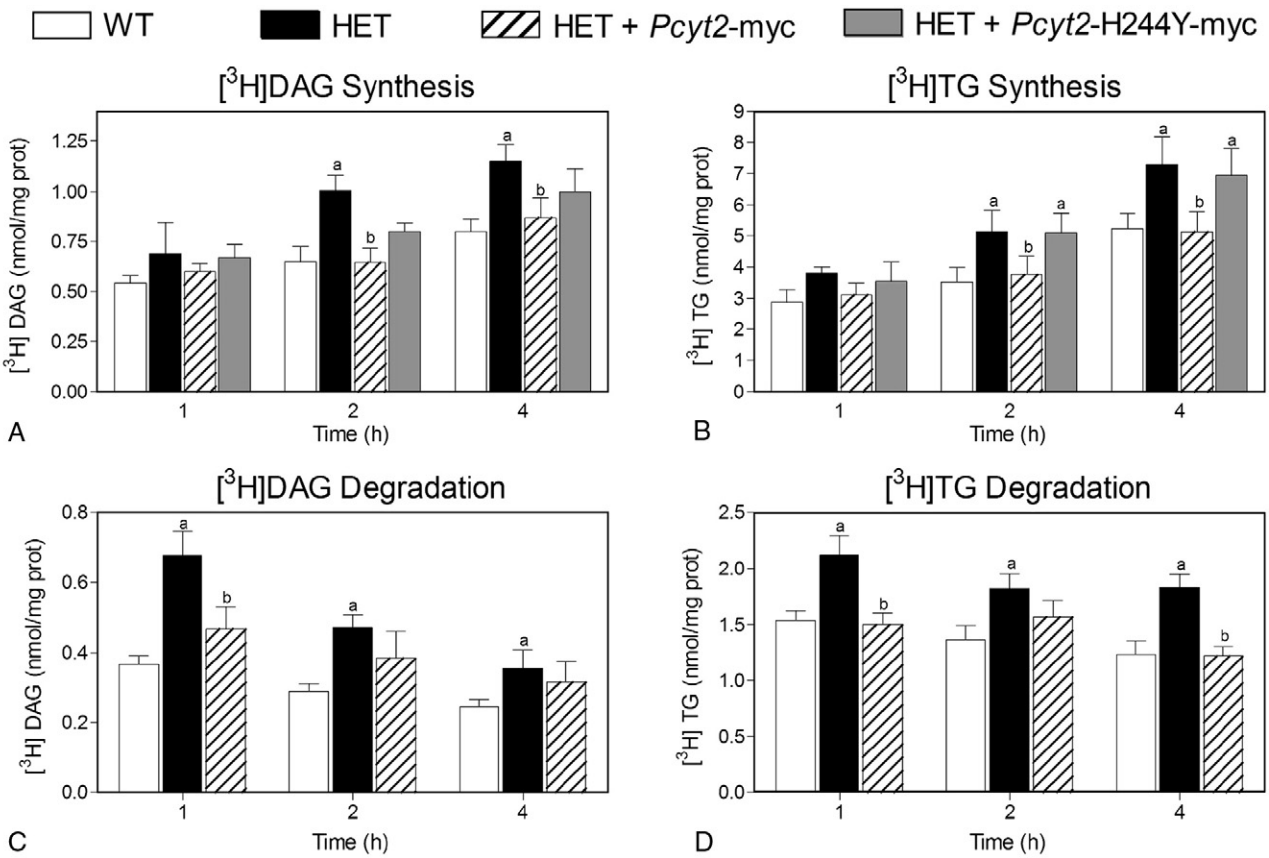

Fig. 3. DAG and TAG turnovers are normalized with Pcyt2 overexpression. WT and HET hepatocytes were transfected for 48 hours and pulse labeled with [^{3}H] glycerol to measure the synthesis of DAG (A) and TAG (B) in transfected and untransfected cells. Pulse-chase labeling with [^{3}H]glycerol to measure degradation of DAG (C) and TAG (D). Time points and transfections are indicated; data are expressed in nanomoles per milligram protein. Hepatocytes are isolated from WT livers (n = 4) and HET livers (n = at least 4 transfected/4 nontransfected), where each time point was performed in triplicate. Significance was established at $P < .05$, where [a] represents a difference relative to WT and [b] represents a difference relative to HET cells as determined by ANOVA.

hepatocytes was related to transfected hepatocytes using an anti-Pcyt2 antibody. Transfected hepatocytes typically demonstrated 2-fold higher expression of the wild-type and H244Y proteins compared with untransfected hepatocytes (Fig. 2A).

3.3. Pcyt2 wild-type but not H244Y mutant normalizes PE metabolism in deficient hepatocytes

Pulse labeling of the PE-Kennedy pathway with [^{14}C] ethanolamine was performed in both transfected and untransfected *Pcyt2*$^{+/-}$ hepatocytes and compared with radiolabeled *Pcyt2*$^{+/+}$ controls. At all time points, it was evident that *Pcyt2*$^{+/-}$ hepatocytes accumulated more [^{14}C] phosphoethanolamine and had reduced formation of [^{14}C] CDP-ethanolamine and [^{14}C]PE compared with control wild-type hepatocytes (Fig. 2B-D), as was previously reported [22,23]. After overexpression of the *Pcyt2*-myc/His (wild-type) plasmid in *Pcyt2*$^{+/-}$ hepatocytes, the PE-Kennedy pathway was normalized at all time points and was more comparable to *Pcyt2*$^{+/+}$ hepatocytes (B-D). At the end of the 4-hour labeling, the transfection of Pcyt2 back into the heterozygous hepatocytes decreased [^{14}C]phosphoethanolamine by 35% and increased [^{14}C]CDP-ethanolamine by 27% (Fig. 2C, D), indicating a compensation of Pcyt2 function. Synthesis of [^{14}C]PE increased 21% in transfected *Pcyt2*$^{+/-}$ hepatocytes and approached the basal value of control hepatocytes (Fig. 2B). On the other hand, transfection of the H244Y mutant did not reduce [^{14}C]phosphoethanolamine or increased [^{14}C]CDP-ethanolamine and [^{14}C]PE in *Pcyt2*$^{+/-}$ hepatocytes (Fig. 2B-D). When pulse experiments were performed with [^{3}H]glycerol, the trends in [^{3}H]PE synthesis (Fig. 2E) directly mimicked that of [^{14}C]PE synthesis from [^{14}C]ethanolamine (Fig. 2D), clearly establishing that the wild-type Pcyt2 but not the H244Y mutant was capable to fully restore the PE synthesis in deficient hepatocytes.

We next performed pulse-chase radiolabeling with [^{3}H] glycerol (Fig. 2F) to study PE degradation. Because the mutant construct was unable to restore PE synthesis (Fig. 2B-D), it was excluded from these experiments. *Pcyt2*$^{+/-}$ hepatocytes were transfected with the *Pcyt2*-myc/His plasmid, and PE degradation was compared with untransfected *Pcyt2*$^{+/-}$ and *Pcyt2*$^{+/+}$ hepatocytes during 4-hour chase (Fig. 2F). [^{3}H]PE in transfected *Pcyt2*$^{+/-}$ hepatocytes resembled [^{3}H]PE of *Pcyt2*$^{+/+}$ controls after 1-hour chase; and [^{3}H]PE declines from 1 to 2 hours were similar, that is,

0.16 and 0.15 nmol/mg, respectively. [^{3}H]PE in untransfected *Pcyt2*$^{+/-}$ hepatocytes was significantly lower after the initial 1-hour chase and became reduced by only 0.02 nmol/mg from 1- to 2-hour chase. Therefore, overexpression of the *Pcyt2*-myc/His plasmid in deficient *Pcyt2*$^{+/-}$ hepatocytes increased PE degradation and made it more comparable to control hepatocytes. When the actual pool sizes of PE were measured, there was no difference among treatments (data not shown), consistent with previous findings [22,23] and with the well-established homeostatic mechanism for the preservation of membrane phospholipids, where increased synthesis is typically balanced by increased degradation and vice versa.

3.4. Pcyt2 wild-type but not H244Y mutant restores DAG and TAG metabolism

In *Pcyt2*$^{+/-}$ mice, metabolic abnormalities develop progressively with age and therefore may or may not be directly related to the impaired PE synthesis via the PE-Kennedy pathway [22]. We hypothesized that if deficiency at the *Pcyt2* locus is directly responsible for the observed fatty liver phenotype and TAG accumulation, restoration of the PE-Kennedy pathway with *Pcyt2* cDNA (Fig. 2) should simultaneously bring DAG and TAG to normal levels. Indeed, upon the overexpression of wild-type Pcyt2 in deficient hepatocytes, the formation of both DAG and TAG decreased to the levels of control hepatocytes, as assessed by [^{3}H]glycerol pulse labeling for 1, 2, and 4 hours (Fig. 3A and B). As in the case of PE synthesis, the Pcyt2 H244Y mutant only partially restored DAG synthesis and had no effect on TAG synthesis (Fig. 3A, B); and it was excluded from further metabolic labeling experiments.

The pulse-chase experiments with [^{3}H]glycerol established that DAG and TAG degradation, which was significantly elevated in *Pcyt2*$^{+/-}$ hepatocytes, became reduced after overexpression of the wild-type plasmid and approached the values of control hepatocytes (Fig. 3C, D). When the actual pool sizes of DAG and TAG were examined by the equilibrium radiolabeling with [^{3}H]glycerol (Fig. 4), Pcyt2 overexpression significantly reduced the total DAG pool relative to untransfected *Pcyt2*$^{+/-}$ hepatocytes (0.87 ± 0.09 vs 1.17 ± 0.12 nmol/mg, $P < .05$); and the levels became very similar to *Pcyt2*$^{+/+}$ control hepatocytes (0.81 ± 0.08 nmol/mg, $P < .03$) (Fig. 4A). The TAG pool size was also reduced by Pcyt2 overexpression; however, it was not

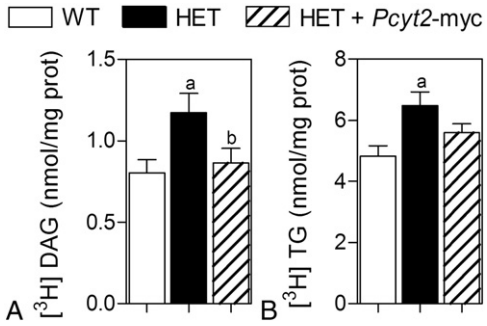

Fig. 4. Reintroduction of Pcyt2 reduced the elevated neutral lipid pools. WT and HET hepatocytes were transfected for 48 hours, and the "steady-state" total cellular pools of DAG (A) and TAG (B) were compared after 24-hour radiolabeling with [^{3}H]glycerol. Data are expressed as nanomoles per milligram protein from WT type (n = 2) and HET (n = 4 transfected/4 nontransfected) hepatocytes, performed in triplicate. Significance was established at $P < .05$, where [a] represents a difference relative to WT and [b] represents a difference relative to HET cells as determined by ANOVA.

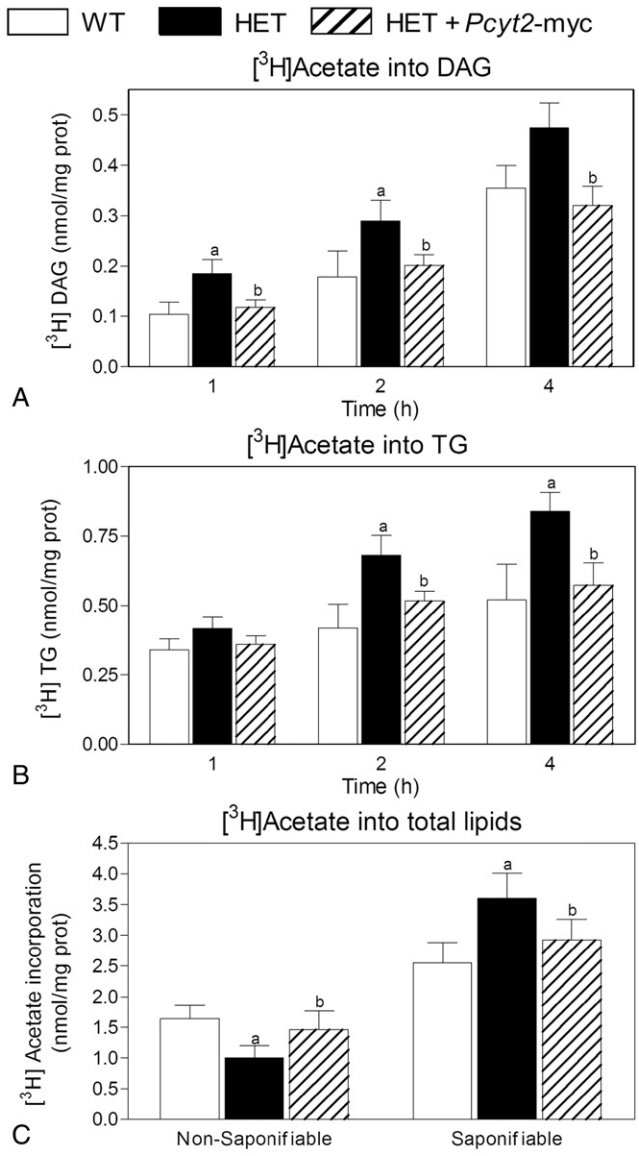

Fig. 5. Increased lipogenesis in deficient hepatocytes is corrected by Pcyt2. The incorporation of [^{3}H]acetate into DAG (A) and TAG (B) as an indication of de novo lipid synthesis after 48-hour transfection. C, [^{3}H] Acetate incorporation into total glycerolipids (nonsaponifiable) and total cholesterol (saponifiable). All data are expressed as nanomoles per milligram protein from WT (n = 2) and HWT (n = 4 transfected/4 nontransfected) hepatocytes, performed in triplicate. Significance was established at $P < .05$, where [a] represents a difference relative to WT and [b] represents a difference relative to HET cells as determined by ANOVA.

statistically different from *Pcyt2*$^{+/-}$ hepatocytes (6.47 ± 0.46 vs 5.59 ± 0.29 nmol/mg) (Fig. 4B).

3.5. Reestablished Pcyt2 reduces lipogenesis in deficient hepatocytes

We used radiolabeling with [^{3}H]acetate to measure the incorporation of newly synthesized fatty acids (lipogenesis) into various lipid fractions (Fig. 5). Relative to *Pcyt2*$^{+/+}$ control cells, *Pcyt2*$^{+/-}$ hepatocytes had significantly elevated [^{3}H]acetate labeling of DAG and TAG as observed initially in vivo [22]. When *Pcyt2* cDNA was introduced into deficient hepatocytes, [^{3}H]DAG and [^{3}H]TAG synthesis returned to the basal levels of control hepatocytes (Fig. 5A, B). When incorporation of [^{3}H]acetate was assessed at the level of total glycerolipids-phospholipids, DAG and TAG, (saponifiable fraction) and total cholesterol (nonsaponifiable fraction), the introduction of the wild-type Pcyt2 corrected the values for both lipids (Fig. 5C), demonstrating that in addition to normalizing PE synthesis, the reintroduction of Pcyt2 also restored lipogenesis and adjusted the balance between glycerolipid and cholesterol synthesis that was distorted in deficient hepatocytes [22].

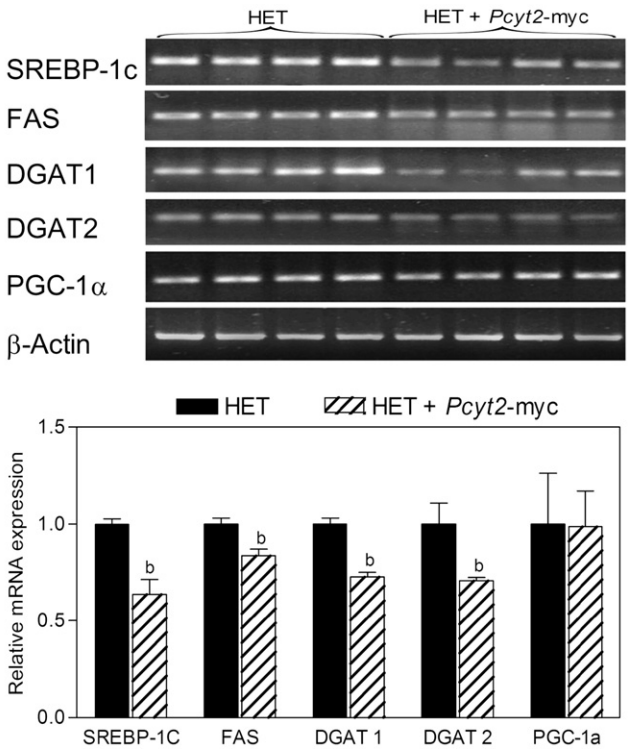

Fig. 6. Expression of lipogenic genes is reduced by Pcyt2. A, Representative data of transcript levels for the lipid genes—*Srebp1c*, *Fas*, *Dgat1*, *Dgat2*, and *PGC1a*—in transfected and nontransfected deficient (HET) hepatocytes. B, Transcript expressions were first normalized to *β*-actin and then expressed relative to nontransfected hepatocytes (n = 2 livers, where each transfection was conducted in quadruplicate and the analyses conducted at least twice); ^{b} represents $P < .05$ as determined by Student *t* test.

3.6. Reestablished Pcyt2 corrects lipogenic gene expression in deficient hepatocytes

We had previously reported that *Pcyt2*$^{+/-}$ mice experience an increased expression of various lipogenic genes [22], yet the initial data did not determine if the effects were directly or indirectly responsive to *Pcyt2* deficiency. Because we established that even transiently transfected *Pcyt2* cDNA normalized lipogenesis and lipid content in deficient hepatocytes, the next logical step was to test if the restored Pcyt2 could, in addition to modifying the metabolite levels, also impact the expression of regulatory lipid genes. As shown in Fig. 6, reintroduction of Pcyt2 into deficient hepatocytes significantly reduced expression of sterol regulatory element binding protein–1c (*Srebp-1c*), a major transcriptional regulator of lipogenesis, and the downstream genes involved in de novo fatty acid (fatty acid synthase [*Fas*]) and TAG synthesis (diacylglycerol acyltransferase 1 and 2 [*Dgat1/2*]), with no alterations in the mitochondrial regulator of fatty acid oxidation–peroxisome proliferator activated receptor coactivator 1α. Together with the metabolic radiolabeling results, these data clearly demonstrated for the first time that Pcyt2 function is critical not only for the PE-Kennedy pathway but also for the regulation of associated pathways involved in liver lipid metabolism.

4. Discussion

Two *Pcyt2* isoforms, α and *β*, typically coexist in the liver and other tissues [15] and are both similarly depleted in *Pcyt2*$^{+/-}$ mice [23]. In this work, we demonstrate that overexpression of a single isoform (α) was able to complement the major metabolic defect of *Pcyt2* gene deficiency, reduced PE synthesis concomitant with increased fat deposition. We further provide direct evidence that *Pcyt2* is also an important antilipogenic gene, necessary to balance membrane PE biogenesis with general fatty acid and glycerolipid metabolism.

In addition to our findings, the association between membrane phospholipids (mainly PC) and TAG homeostasis has been previously noted in cultured cells [26-28]; however, the homozygous or heterozygous disruption in mice of the genes *Pcyt1* or *Pemt* (responsible for PC synthesis) does not result in obesity or perturbations in lipogenesis [29]. It is also interesting that diacylglycerol acyltransferase (DGAT1) knockout mice have normal phospholipids [30]; however, DGAT1 overexpression in human lung fibroblasts caused a reduction in phospholipid synthesis (PE and PC) [31]. Deletion of mitochondrial glycerol-3-phosphate acyltransferase, which catalyzes the first committed step in all glycerolipid (PC, PE, DAG, and TAG) synthesis, resulted in an alteration in fatty acid composition, but not phospholipid content [32]. Finally, deletion of stearoyl–coenzyme A desaturase 1, the rate-limiting enzyme in monounsaturated fatty acid synthesis and the critical regulator of TAG

synthesis, resulted in increases in PC and PE content [33]. *Pcyt2*$^{+/-}$ mice represent the first phospholipid-glycerolipid model clearly demonstrating how systemic impairment in membrane PE (phospholipid) synthesis could disturb TAG homeostasis and gradually lead to development of obesity, fatty liver, hypertriglyceridemia, and insulin resistance, some of the major features of the human metabolic syndrome [22].

The main link between PE and TAG metabolism is the common intermediate DAG; but even though our initial work indicated that DAG not used in the PE-Kennedy pathway is the key to the development of the metabolic syndrome phenotype in *Pcyt2*$^{+/-}$ mice [22], it remained unclear how reduced PE synthesis would result in increased lipogenesis and perpetuated production of DAG and fatty acids from glucose. By returning PE synthesis to normal by overexpression of the wild-type Pcyt2 but not the H244Y mutant, we clearly established that DAG destined for the PE-Kennedy pathway was used for TG formation in deficient hepatocytes. However, because additional fatty acids are required to eliminate excess DAG to form TAG, the need for more fatty acids in deficient hepatocytes was facilitated by de novo lipogenic pathways. Altered expression of genes involved in glucose metabolism (unpublished results) likely contributed to more glycerol-3-phosphate for elevated DAG synthesis. Importantly, the elevated DAG and fatty acid production and the up-regulated lipogenic gene expression in the deficient state were all returned to normal after Pcyt2 function was completely reinstalled, although protein expression of the lipogenic genes is to be determined in future studies.

Although the mechanism by which Pcyt2 may regulate the expression of *Srebp-1c* in heterozygous hepatocytes is not clear, our results indicate a reciprocal relationship whereby it may be possible that *Srebp-1c* expression would be increased in response to the lipid intermediates formed by *Pcyt2* gene disruption, the excess DAG, and/or a need for extra fatty acids to store DAG in the form of TAG. *Srebp-1c* is generally established as the key regulator of lipogenesis in response to insulin signaling. However, we performed experiments in isolated hepatocytes and therefore in the absence of insulin, demonstrating that *Srebp-1c* and lipogenesis are elevated in deficient hepatocytes in the absence of insulin and then reduced in a direct response to the overexpression of Pcyt2. In addition, the functionality of Pcyt2 has a direct influence on the expression of *Dgat1* and *Dgat2*, which could be separated from the regulation of *Srebp-1c* because they are not considered as *Srebp-1c* responsive genes [34,35].

Recently, a liver-specific *Pcyt2* knockout mouse has been developed [36] that has an identical, yet more exaggerated, fatty liver phenotype. Even though liver TAG levels were highly elevated, this mouse model did not develop obesity and other characteristics of the metabolic syndrome. On the other hand, in the model used in this study, a systemic disruption of a single *Pcyt2* allele gradually caused development of an array of consequences, including obesity and insulin resistance [22], suggesting that *Pcyt2* deficiency in other organs, perhaps mostly in adipocytes and muscle, contributed to the overall disease development. It is well known that DAG inhibits insulin signaling [37]; therefore, in *Pcyt2*$^{+/-}$ mice, the observed reduction of DAG levels with *Pcyt2* overexpression could potentially improve insulin signaling in vivo. To establish if reconstitution of Pcyt2 in the deficient mice would further normalize PE, DAG, and TAG metabolism in other tissues, we attempted to generate *Pcyt2* transgenic mice; however, we were unsuccessful in 2 attempts. Therefore, the direct role of *Pcyt2* deficiency in progressive development of insulin resistance, specific for the *Pcyt2* heterozygous state, could not be addressed. The results of the current investigation, however, demonstrate the existence of a direct functional/genetic coupling between *Pcyt2*, lipogenesis, and TAG accumulation. We demonstrate that DAG- and TAG-related fatty liver disorders could originate from impairments in membrane phospholipid homeostasis regulated by the PE-Kennedy pathway, where functional restoration by Pcyt2 in heterozygous hepatocytes reverses the liver metabolic phenotype.

Acknowledgment

This work was supported by an operating grant from the Canadian Institutes of Health Research (grant MOP-177089) to MB.

References

[1] Bakovic M, Fullerton MD, Michel V. Metabolic and molecular aspects of ethanolamine phospholipid biosynthesis: the role of CTP:phosphoethanolamine cytidylyltransferase (Pcyt2). Biochem Cell Biol 2007;85:283-300.

[2] Borkenhagen LF, Kennedy EP, Fielding L. Enzymatic formation and decarboxylation of phosphatidylserine. J Biol Chem 1961;236: PC28-PC30.

[3] Voelker DR, Frazier JL. Isolation and characterization of a Chinese hamster ovary cell line requiring ethanolamine or phosphatidylserine for growth and exhibiting defective phosphatidylserine synthase activity. J Biol Chem 1986;261:1002-8.

[4] Kennedy EP, Weiss SB. The function of cytidine coenzymes in the biosynthesis of phospholipids. J Biol Chem 1956;222:193-214.

[5] Sundler R. Ethanolaminephosphate cytidylyltransferase. Purification and characterization of the enzyme from rat liver. J Biol Chem 1975;250:8585-90.

[6] Bladergroen BA, van Golde LM. CTP:phosphoethanolamine cytidylyltransferase. Biochim Biophys Acta 1997;1348:91-9.

[7] van Hellemond JJ, Slot JW, Geelen MJ, et al. Ultrastructural localization of CTP:phosphoethanolamine cytidylyltransferase in rat liver. J Biol Chem 1994;269:15415-8.

[8] Vermeulen PS, Geelen MJ, van Golde LM. Substrate specificity of CTP: phosphoethanolamine cytidylyltransferase purified from rat liver. Biochim Biophys Acta 1994;1211:343-9.

[9] Vermeulen PS, Tijburg LB, Geelen MJ, et al. Immunological characterization, lipid dependence, and subcellular localization of CTP:phosphoethanolamine cytidylyltransferase purified from rat liver. Comparison with CTP:phosphocholine cytidylyltransferase. J Biol Chem 1993;268:7458-64.

[10] Min-Seok R, Kawamata Y, Nakamura H, et al. Isolation and characterization of ECT1 gene encoding CTP: phosphoethanolamine

cytidylyltransferase of *Saccharomyces cerevisiae*. J Biochem (Tokyo) 1996;120:1040-7.
[11] Nakashima A, Hosaka K, Nikawa J. Cloning of a human cDNA for CTP-phosphoethanolamine cytidylyltransferase by complementation in vivo of a yeast mutant. J Biol Chem 1997;272:9567-72.
[12] Bladergroen BA, Houweling M, Geelen MJ, et al. Cloning and expression of CTP:phosphoethanolamine cytidylyltransferase cDNA from rat liver. Biochem J 1999;343(Pt 1):107-14.
[13] Poloumienko A, Cote A, Quee AT, et al. Genomic organization and differential splicing of the mouse and human Pcyt2 genes. Gene 2004;325:145-55.
[14] Park YS, Gee P, Sanker S, et al. Identification of functional conserved residues of CTP:glycerol-3-phosphate cytidylyltransferase. Role of histidines in the conserved HXGH in catalysis. J Biol Chem 1997;272: 15161-6.
[15] Tie A, Bakovic M. Alternative splicing of CTP:phosphoethanolamine cytidylyltransferase produces two isoforms that differ in catalytic properties. J Lipid Res 2007;48:2172-81.
[16] Johnson CM, Yuan Z, Bakovic M. Characterization of transcription factors and cis-acting elements that regulate human CTP: phosphoethanolamine cytidylyltransferase (Pcyt2). Biochim Biophys Acta 2005;1735:230-5.
[17] Zhu L, Johnson C, Bakovic M. Stimulation of the human CTP: phosphoethanolamine cytidylyltransferase gene by early growth response protein 1. J Lipid Res 2008;49:2197-211.
[18] Zhu L, Michel V, Bakovic M. Regulation of the mouse CTP: phosphoethanolamine cytidylyltransferase gene Pcyt2 during myogenesis. Gene 2009;447:51-9.
[19] Sundler R, Akesson B. Regulation of phospholipid biosynthesis in isolated rat hepatocytes. Effect of different substrates. J Biol Chem 1975;250:3359-67.
[20] Lykidis A, Wang J, Karim MA, et al. Overexpression of a mammalian ethanolamine-specific kinase accelerates the CDP-ethanolamine pathway. J Biol Chem 2001;276:2174-9.
[21] Tijburg LB, Houweling M, Geelen MJ, et al. Inhibition of phosphatidylethanolamine synthesis by glucagon in isolated rat hepatocytes. Biochem J 1989;257:645-50.
[22] Fullerton MD, Hakimuddin F, Bonen A, et al. The development of a metabolic disease phenotype in CTP:phosphoethanolamine cytidylyltransferase–deficient mice. J Biol Chem 2009;284:25704-13.
[23] Fullerton MD, Hakimuddin F, Bakovic M. Developmental and metabolic effects of disruption of the mouse CTP:phosphoethanolamine cytidylyltransferase gene (Pcyt2). Mol Cell Biol 2007;27: 3327-36.
[24] Bligh EG, Dyer WJ. A rapid method of total lipid extraction and purification. Can J Biochem Physiol 1959;37:911-7.
[25] Tijburg LB, Vermeulen PS, van Golde LM. Ethanolamine-phosphate cytidylyltransferase. Methods Enzymol 1992;209:258-63.
[26] Caviglia JM, De Gomez Dumm IN, Coleman RA, et al. Phosphatidylcholine deficiency upregulates enzymes of triacylglycerol metabolism in CHO cells. J Lipid Res 2004;45:1500-9.
[27] Guo Y, Walther TC, Rao M, et al. Functional genomic screen reveals genes involved in lipid-droplet formation and utilization. Nature 2008;453:657-61.
[28] Igal RA, Coleman RA. Neutral lipid storage disease: a genetic disorder with abnormalities in the regulation of phospholipid metabolism. J Lipid Res 1998;39:31-43.
[29] Vance DE. Role of phosphatidylcholine biosynthesis in the regulation of lipoprotein homeostasis. Curr Opin Lipidol 2008;19:229-34.
[30] Smith SJ, Cases S, Jensen DR, et al. Obesity resistance and multiple mechanisms of triglyceride synthesis in mice lacking Dgat. Nat Genet 2000;25:87-90.
[31] Bagnato C, Igal RA. Overexpression of diacylglycerol acyltransferase-1 reduces phospholipid synthesis, proliferation, and invasiveness in simian virus 40–transformed human lung fibroblasts. J Biol Chem 2003;278:52203-11.
[32] Hammond LE, Gallagher PA, Wang S, et al. Mitochondrial glycerol-3-phosphate acyltransferase–deficient mice have reduced weight and liver triacylglycerol content and altered glycerolipid fatty acid composition. Mol Cell Biol 2002;22:8204-14.
[33] Dobrzyn A, Dobrzyn P, Miyazaki M, et al. Stearoyl-CoA desaturase 1 deficiency increases CTP:choline cytidylyltransferase translocation into the membrane and enhances phosphatidylcholine synthesis in liver. J Biol Chem 2005;280:23356-62.
[34] Choi CS, Savage DB, Kulkarni A, et al. Suppression of diacylglycerol acyltransferase-2 (DGAT2), but not DGAT1, with antisense oligonucleotides reverses diet-induced hepatic steatosis and insulin resistance. J Biol Chem 2007;282:22678-88.
[35] Villanueva CJ, Monetti M, Shih M, et al. Specific role for acyl CoA: diacylglycerol acyltransferase 1 (Dgat1) in hepatic steatosis due to exogenous fatty acids. Hepatology 2009;50:434-42.
[36] Leonardi R, Frank MW, Jackson PD, et al. Elimination of the CDP-ethanolamine pathway disrupts hepatic lipid homeostasis. J Biol Chem 2009;284:27077-89.
[37] Yu C, Chen Y, Cline GW, et al. Mechanism by which fatty acids inhibit insulin activation of insulin receptor substrate-1 (IRS-1)–associated phosphatidylinositol 3-kinase activity in muscle. J Biol Chem 2002;277:50230-6.